

We are IntechOpen, the world's leading publisher of Open Access books Built by scientists, for scientists

4,800

Open access books available

122,000

International authors and editors

135M

Downloads

Our authors are among the

154

Countries delivered to

TOP 1%

most cited scientists

12.2%

Contributors from top 500 universities



WEB OF SCIENCE™

Selection of our books indexed in the Book Citation Index
in Web of Science™ Core Collection (BKCI)

Interested in publishing with us?
Contact book.department@intechopen.com

Numbers displayed above are based on latest data collected.

For more information visit www.intechopen.com



Coherent Spin Dependent Transport in QD-DTJ Systems

Minjie Ma¹, Mansoor Bin Abdul Jalil^{1,2} and Seng Ghee Tan^{1,3}

¹Computational Nanoelectronics and Nano-Device Laboratory, Electrical and Computer Engineering Department, National University of Singapore

²Information Storage Materials Laboratory, Department of Electrical and Computer Engineering, National University of Singapore

³Data Storage Institute, A *STAR (Agency of Science, Technology and Research) Singapore

1. Introduction

As the dimension of devices reduces to nano-scale regime, the spin-dependent transport (SDT) and spin effects in quantum dot (QD) based systems become significant. These QD based systems have attracted much interest, and can potentially be utilized for spintronic device applications. In this chapter, we consider nano-scale spintronic devices consisting of a QD with a double barrier tunnel junction (QD-DTJ)(schematically shown in Fig. 1). The DTJ couples the QD to two adjacent leads which can be ferromagnetic (FM) or non-magnetic (NM).

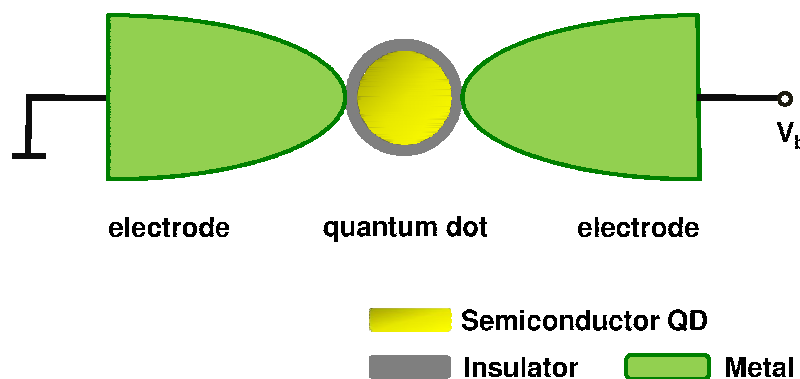


Fig. 1. QD-DTJ system consists of a QD coupling to two electrodes via double tunnel junctions. V_b is the bias voltage, under which the electrons tunnel through the QD one by one.

In a QD-DTJ system, the electron tunneling is affected by the quantized energy levels of the QD, and can thus be referred to as single electron tunneling. The single electron tunneling process becomes spin-dependent when the leads or the QD is a spin polarizer, where the density of states (DOS) for spin-up and spin-down electrons are different. The interplay of SDT with quantum and/or single electron charging effects makes the QD-DTJ systems interesting. In such QD-DTJ systems, it is possible to observe several quantum spin phenomena, such as spin blockade (Shaji et al. (2008)), Coulomb

blockade (CB) (Bruus & Flensberg (2004)), cotunneling (Weymann & Barnaś (2007)), tunnel magnetoresistance (TMR) (Rudziński & Barnaś (2001)), spin transfer torque (Mu et al. (2006)) and Kondo effect (Katsura (2007); Lobo et al. (2006); Potok et al. (2007)). The complex spin and charge transport properties of QD-DTJ systems have attracted extensive theoretical (Bao et al. (2008); Braig & Brouwer (2005); Jauho et al. (1994); Kuo & Chang (2007); Ma et al. (2008); Meir & Wingreen (1992); Meir et al. (1991; 1993); Mu et al. (2006); Qi et al. (2008); Qu & Vasilopoulos (2006); Souza et al. (2004); Zhang et al. (2002); Zhu & Balatsky (2002)) and experimental ((Deshmukh & Ralph, 2002; Hamaya et al., 2007; Pasupathy et al., 2004; Potok et al., 2007)) investigations recently. These studies may ultimately lead to the utilization of such devices in diverse applications such as single spin detector (Wabnig & Lovett (2009)) and STM microscopy (Manassen et al. (2001)).

The theoretical study of the SDT through these DTJ systems are mainly based on two approaches, namely the master equation (ME) approach and the Keldysh nonequilibrium Green's function (NEGF) approach. For coherent transport across QD-DTJ devices, quantum transport methods are applied, such as the linear response (Kubo) method applicable for small bias voltage, and its generalization, the NEGF method for arbitrary bias voltage. Since the objective of the study in this Chapter is for device application over a wide voltage range, we focus on the latter. The NEGF method has been employed to analyze various transport properties of QD-DTJ systems, such as TMR, tunneling current (Weymann & Barnaś (2007)) and conductance. These analyses were conducted based on the Anderson model (Meir et al. (1993); Qi et al. (2008)), for collinear or noncollinear (Mu et al. (2006); Sergueev et al. (2002); Weymann & Barnaś (2007)) configurations of the magnetization of the two FM leads, or in the presence of spin-flip scattering in the QD (Lin & D.-S.Chuu (2005); Souza et al. (2004); Zhang et al. (2002)).

In this Chapter, based on the NEGF approach, we study the SDT through two QD-DTJ systems. In Section. 2, the electronic SDT through a single energy-level QD-DTJ is theoretically studied, where the two FM leads enable the electron transport spin-dependent. In the study, we systematically incorporate the effect of the spin-flip (SF) within the QD and the SF during tunneling the junction between the QD and each lead, and consider possible asymmetry between the coupling strengths of the two tunnel junctions. Based on the theoretical model, we first investigate the effects of both types of SF events on the tunneling current and TMR; subsequently, we analyze the effect of coupling asymmetry on the QD's electron occupancies and the charge and spin currents through the system (Ma et al. (2010)).

In Section. 3, we studied the SDT through a QD-DTJ system with finite Zeeman splitting (ZS) in the QD, where the two leads which sandwich the QD are NM. The spin-dependence of the electron transport is induced by the ZS caused by the FM gate attached to the QD. A fully polarized tunneling current is expected through this QD-DTJ system. The charge and spin currents are to be analyzed for the QD-DTJ systems with or without ZS.

2. Single energy level QD

The QD-DTJ device under consideration is shown in Fig. 2. It consists of two FM leads and a central QD in which a single energy level is involved in the electron tunneling process. The SDT through the QD-DTJ is to be theoretically modeled via the Keldysh NEGF approach (Caroli et al. (1971); Meir & Wingreen (1992)). In the transport model, the limit of small correlation energy is assumed, in the case where the energy due to electron-electron

interaction in the QD is much smaller than the thermal energy or the separation between the discrete energy levels in the QD (Fransson & Zhu (2008)).

2.1 Theory

For the QD-DTJ device shown in Fig. 2, the full Hamiltonian consists of the lead Hamiltonian H_α , the QD Hamiltonian H_d , and the tunneling Hamiltonian H_t . The explicit form of the Hamiltonian is given by

$$H = \sum_{\alpha} H_{\alpha} + H_d + H_t, \quad (1)$$

where

$$H_{\alpha} = \sum_{k\sigma} \epsilon_{\alpha k\sigma} a_{\alpha k\sigma}^{\dagger} a_{\alpha k\sigma}, \quad (2)$$

$$H_d = \sum_{\sigma} \epsilon_{\sigma\sigma} a_{\sigma}^{\dagger} a_{\sigma} + \sum_{\sigma} \epsilon_{\sigma\bar{\sigma}} a_{\bar{\sigma}}^{\dagger} a_{\sigma}, \quad (3)$$

$$H_t = \sum_{\alpha k\sigma} \left(t_{\alpha k\sigma, \sigma} a_{\sigma}^{\dagger} a_{\alpha k\sigma} + t_{\alpha k\sigma, \sigma}^* a_{\alpha k\sigma}^{\dagger} a_{\sigma} \right) + \sum_{\alpha k\sigma} \left(t_{\alpha k\sigma, \bar{\sigma}} a_{\bar{\sigma}}^{\dagger} a_{\alpha k\sigma} + t_{\alpha k\sigma, \bar{\sigma}}^* a_{\alpha k\sigma}^{\dagger} a_{\bar{\sigma}} \right). \quad (4)$$

In the above, $\epsilon_{\sigma\sigma}$ is the single energy level in the QD, $\epsilon_{\sigma\bar{\sigma}}$ denotes the coupling energy of the spin-flip within quantum dot (SF-QD) from spin- σ to spin- $\bar{\sigma}$ state, $t_{\alpha k\sigma, \sigma}$ ($t_{\alpha k\sigma, \bar{\sigma}}$) is the coupling between electrons of the same (opposite) spin states in the lead and the QD. $\alpha = \{L, R\}$ is the lead index for the left and right leads, $\sigma = \{\uparrow, \downarrow\}$ stands for up- and down-spin, and k is the momentum, $\epsilon_{\alpha k\sigma}$ represents the energy in the leads. The operators a_{ν}^{\dagger} (a_{ν}) and a_{σ}^{\dagger} (a_{σ}) are the creation (annihilation) operators for the electrons in the leads and the QD, respectively.

2.1.1 Tunneling current and tunnel magnetoresistance

The tunneling current through the QD-DTJ system can be expressed as the rate of change of the occupation number $N = \sum_{\sigma} a_{\sigma}^{\dagger} a_{\sigma}$ in the QD,

$$I = e\dot{N} = \frac{ie}{\hbar} \langle [H, N] \rangle. \quad (5)$$

Without loss of generality, we can calculate the tunneling current in Eq. (5) by considering the tunneling current I_L through the left junction between the left lead and the QD. Evaluating the commutator in Eq. (5) in terms of creation and annihilation operators gives

$$I = I_L = \frac{ie}{\hbar} \sum_{Lk\sigma, \sigma'} \left(t_{Lk\sigma, \sigma'} \langle a_{Lk\sigma}^{\dagger} a_{\sigma'} \rangle - t_{Lk\sigma, \sigma'}^* \langle a_{\sigma'}^{\dagger} a_{Lk\sigma} \rangle \right). \quad (6)$$

In Eq. (6), one may replace the creation and annihilation operators by the lesser Green's functions, which are defined as $G_{\sigma', Lk\sigma}^<(t) = i \langle a_{Lk\sigma}^{\dagger} a_{\sigma'}(t) \rangle$ and $G_{Lk\sigma, \sigma'}^<(t) = i \langle a_{\sigma'}^{\dagger} a_{Lk\sigma}(t) \rangle$ (Meir & Wingreen (1992)). Eq. (6) then takes the form of

$$I_L = \frac{e}{\hbar} \sum_{Lk\sigma, \sigma'} \left(t_{Lk\sigma, \sigma'} G_{\sigma', Lk\sigma}^<(t) - t_{Lk\sigma, \sigma'}^* G_{Lk\sigma, \sigma'}^<(t) \right). \quad (7)$$

After performing a Fourier transform on Eq. (7), $G_{Lk\sigma, \sigma'}^<(\epsilon)$ can be expressed in form of the left lead's and QD's Green's functions, under the assumption of non-interacting

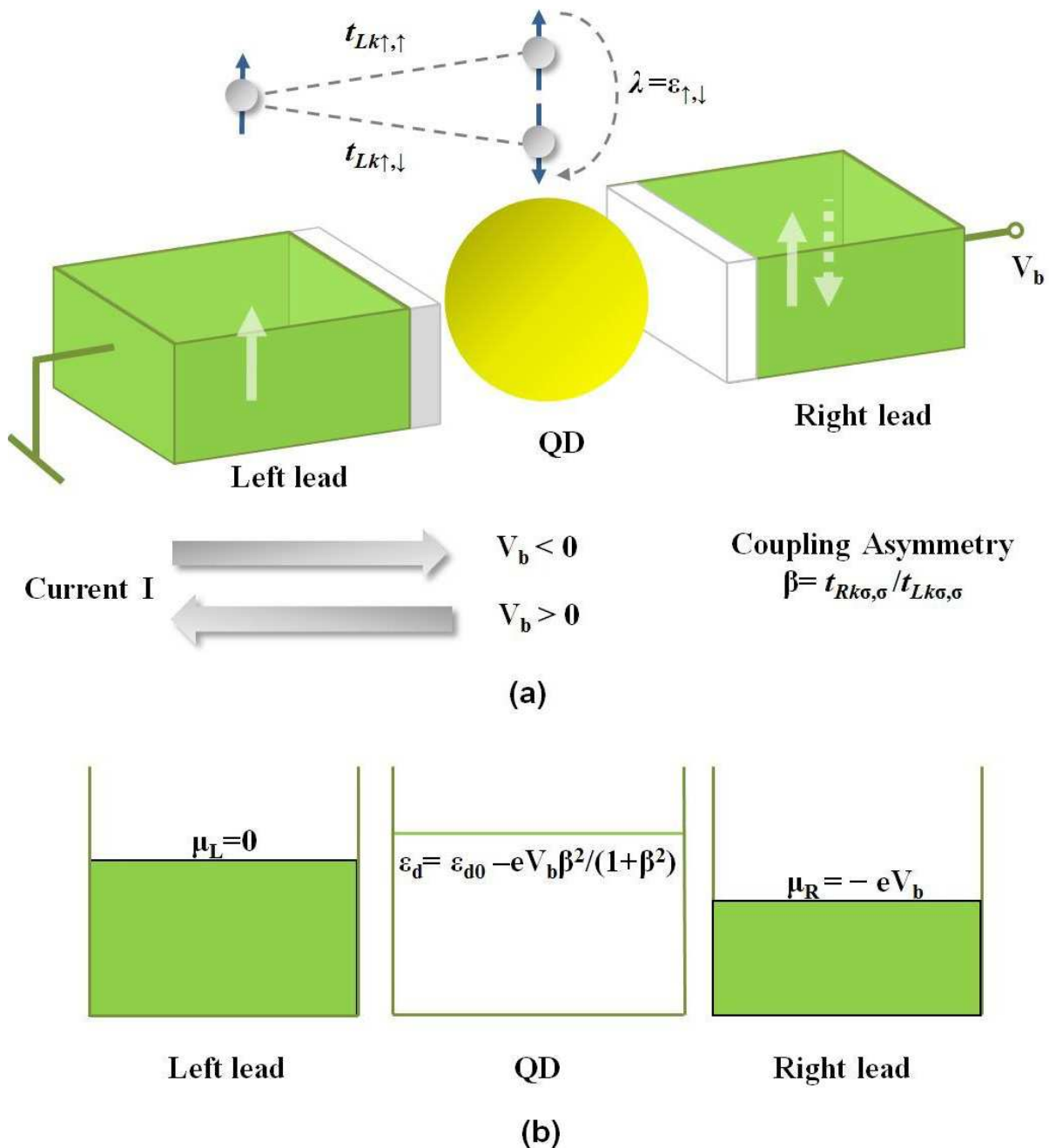


Fig. 2. (a) Schematic diagram of the QD-DTJ structure consisting of a QD sandwiched by two FM leads; (b) the schematic energy diagram for the system in (a). In (a), the arrows in the leads indicate magnetization directions, which can either be in parallel (solid) or antiparallel (dashed) configuration, V_b denotes the bias between the two leads, λ characterizes the strength of the SF-QD, $t_{Lk\uparrow,\downarrow}$ describes the SF-TJ from the up-spin state in left lead and the down-spin state in the QD, $t_{Lk\uparrow,\uparrow}$ shows the coupling between the same electron spin states in left lead and QD, and $\beta = t_{Rk\sigma,\sigma} / t_{Lk\sigma,\sigma}$ represents the coupling asymmetry between the left and right tunneling junctions. In (b), μ_L and μ_R are the chemical potentials of left and right leads respectively, and ϵ_d (ϵ_{d0}) denotes the single energy level of the QD with or without bias voltage.

leads. Taking into account the contour-ordered integration over the time loop, the corresponding Dyson's equations for $G_{Lk\sigma,\sigma'}^<(\epsilon)$ can then be obtained (Mahan (1990)), i.e., $G_{Lk\sigma,\sigma'}^<(\epsilon) = \sum_{\sigma''} t_{Lk\sigma,\sigma''} [g_{Lk\sigma,Lk\sigma'}^t(\epsilon) G_{\sigma'',\sigma'}^<(\epsilon) - g_{Lk\sigma,Lk\sigma'}^<(\epsilon) G_{\sigma'',\sigma'}^{\bar{t}}(\epsilon)]$ and $G_{\sigma',Lk\sigma}^<(\epsilon) = \sum_{\sigma''} t_{Lk\sigma,\sigma''}^* [g_{Lk\sigma,Lk\sigma'}^<(\epsilon) G_{\sigma'',\sigma'}^t(\epsilon) - g_{Lk\sigma,Lk\sigma'}^{\bar{t}}(\epsilon) G_{\sigma'',\sigma'}^<(\epsilon)]$, where $G^t = \theta(t)G^> + \theta(-t)G^<$ and $G^{\bar{t}} = \theta(-t)G^> + \theta(t)G^<$ are the time-ordered and anti-time-ordered Green's functions respectively, $G_{\sigma',\sigma'}^<(t) = -i\langle a_{\sigma'}^\dagger a_{\sigma'}(t) \rangle$, and the g 's are the corresponding unperturbed Green's functions of the leads, whose lesser Green's function and greater Green's function are in form of $g_{Lk\sigma,Lk\sigma'}^<(\epsilon) = i2\pi f_{L\sigma}(\epsilon)\delta(\epsilon - \epsilon_{L\sigma})$ and $g_{Lk\sigma,Lk\sigma'}^>(\epsilon) = -i2\pi[1 - f_{L\sigma}(\epsilon)]\delta(\epsilon - \epsilon_{L\sigma})$, where $f_{L\sigma}(\epsilon) = (1 + \exp(\frac{\epsilon - \mu_L}{k_B T}))^{-1}$ is the Fermi-Dirac function, μ_L is the chemical potential, $\epsilon_{L\sigma}$ is the energy for electrons with spin σ in the left lead, k_B is the Boltzmann constant and T is the temperature of the device. With this, the current in Eq. (7) can be expressed in terms of the Green's functions wholly of the leads and the QD, i.e.,

$$I_L = \frac{e}{\hbar} \sum_{Lk\sigma,\sigma'} \int_{-\infty}^{\infty} \frac{d\epsilon}{2\pi} \{ t_{Lk\sigma,\sigma'} \sum_{\sigma''} t_{Lk\sigma,\sigma''}^* [g_{Lk\sigma,Lk\sigma'}^<(\epsilon) G_{\sigma'',\sigma'}^t(\epsilon) - g_{Lk\sigma,Lk\sigma'}^{\bar{t}}(\epsilon) G_{\sigma'',\sigma'}^<(\epsilon)] - t_{Lk\sigma,\sigma'}^* \sum_{\sigma''} t_{Lk\sigma,\sigma''} [g_{Lk\sigma,Lk\sigma'}^t(\epsilon) G_{\sigma'',\sigma'}^<(\epsilon) - g_{Lk\sigma,Lk\sigma'}^<(\epsilon) G_{\sigma'',\sigma'}^{\bar{t}}(\epsilon)] \}. \tag{8}$$

By applying the identities $G^t + G^{\bar{t}} = G^< + G^>$ and $G^> - G^< = G^r - G^a$ to Eq. (8), we obtain after some algebra (Mahan (1990)):

$$I_L = \frac{ie}{\hbar} \sum_{Lk\sigma,\sigma'} \int_{-\infty}^{\infty} \frac{d\epsilon}{2\pi} t_{Lk\sigma,\sigma'} |_{\epsilon=\epsilon_v} t_{Lk\sigma,\sigma''}^* |_{\epsilon=\epsilon_v} \{ f_v(\epsilon) [G_{\sigma',\sigma''}^r(\epsilon) - G_{\sigma',\sigma''}^a(\epsilon)] + G_{\sigma',\sigma''}^<(\epsilon) \}. \tag{9}$$

We now introduce the density of states for the electrons in the FM leads, denoted by $\rho_{\alpha\sigma}(\epsilon)$. For the electrons in the left FM lead, the density of states is $\rho_{L\sigma}(\epsilon) = [1 + (-1)^\sigma p_L] \rho_{L0}(\epsilon)$, while for the electrons in the right FM lead, it is $\rho_{R\sigma}(\epsilon) = [1 + (-1)^{a+\sigma} p_R] \rho_{R0}(\epsilon)$, where $\sigma = \{0, 1\}$ for spin-up/down electrons, $a = \{0, 1\}$ for parallel/antiparallel alignment of the two FM leads' magnetization, $\rho_{\alpha 0} = (\rho_{\alpha\uparrow} + \rho_{\alpha\downarrow}) / 2$, and p_α is the polarization of the lead α . For the summation over k in Eq.(9), one may apply the continuous limit approximation $\sum_{\{Lk\sigma\}} \rightarrow \sum_{\{L\sigma\}} \int d\epsilon \rho_{L\sigma}(\epsilon)$. The current then can be expressed as

$$I_L = \frac{ie}{\hbar} \sum_{v=\{L\sigma\}} \int d\epsilon \text{tr} \{ f_v(\epsilon) \Gamma_v [G^r(\epsilon) - G^a(\epsilon)] + \Gamma_v G^<(\epsilon) \}, \tag{10}$$

where Γ_v and $G^{(r,a,<)}(\epsilon)$ are (2×2) coupling and Green's function matrices, given by

$$\Gamma_{L\sigma}(\epsilon) = 2\pi\rho_{L\sigma}(\epsilon) \begin{pmatrix} |t_{L\sigma,\sigma}(\epsilon)|^2 & |t_{L\sigma,\sigma}^*(\epsilon)t_{L\sigma,\bar{\sigma}}(\epsilon)| \\ |t_{L\sigma,\bar{\sigma}}^*(\epsilon)t_{L\sigma,\sigma}(\epsilon)| & |t_{L\sigma,\bar{\sigma}}^*(\epsilon)t_{L\sigma,\bar{\sigma}}(\epsilon)| \end{pmatrix}, \tag{11}$$

$$G^{(r,a,<)}(\epsilon) = \begin{pmatrix} G_{\sigma,\sigma}^{(r,a,<)}(\epsilon) & G_{\bar{\sigma},\sigma}^{(r,a,<)}(\epsilon) \\ G_{\sigma,\bar{\sigma}}^{(r,a,<)}(\epsilon) & G_{\bar{\sigma},\bar{\sigma}}^{(r,a,<)}(\epsilon) \end{pmatrix}. \tag{12}$$

In Eq.(11), $t_{L\sigma,\sigma}(t_{L\sigma,\bar{\sigma}})$ applies for the case of spin- σ electron tunneling to the spin- σ ($\bar{\sigma}$) state with (without) spin-flip. In low-bias approximation, $\Gamma_{L\sigma}(\epsilon)=2\pi\rho_{L\sigma}(\epsilon)|t_{L\sigma,\sigma'}^*(\epsilon)t_{L\sigma,\sigma''}(\epsilon)|$ is taken to be constant (zero) within (beyond) the energy range close to the lead's electrochemical potential where most of the transport occurs, i.e., $\epsilon \in [\mu_\alpha - D, \mu_\alpha + D]$, where D is constant (Bruus & Flensberg (2004)). Based on the kinetic equation (Meir & Wingreen (1992)), the lesser Green's function $G_{\sigma',\sigma''}^<(\epsilon)$ can be written as $G_{\sigma',\sigma''}^<(\epsilon) = iG_{\sigma',\sigma''}^r(\epsilon)G_{\sigma',\sigma''}^a(\epsilon)[\Gamma_{L\sigma}f_{L\sigma}(\epsilon) + \Gamma_{R\sigma}f_{R\sigma}(\epsilon)]$, where $G_{\sigma',\sigma''}^r(t) = -i\theta(t)\langle\{a_{\sigma'},^\dagger a_{\sigma''}(t)\}\rangle$ and the advanced Green's function $G_{\sigma',\sigma''}^a(\epsilon) = [G_{\sigma',\sigma''}^r(\epsilon)]^*$. $\Gamma_{\alpha\sigma}$ is the aforementioned coupling strength, and $f_{\alpha\sigma} = \left(1 + \exp\left(\frac{\epsilon - \mu_{\alpha\sigma}}{k_B T}\right)\right)^{-1}$ is the Fermi-Dirac function of lead α , with $\mu_{\alpha\sigma}$ being the chemical potential of that lead. When a bias voltage of V_b is between the two leads, the leads' electrochemical potentials are, respectively, given by $\mu_{L\sigma} = 0$ and $\mu_{R\sigma} = -eV_b$.

Considering that the current from the left lead to the QD is equal to the current from the QD to the right lead, one may calculate the current in a symmetric form, i.e., $I = \frac{I_L + I_R}{2}$. The final form for the total current is then given by

$$I = \frac{e}{h} \sum_{\sigma} \int d\epsilon [f_{L\sigma}(\epsilon) - f_{R\sigma}(\epsilon)] \text{tr}\{\mathbf{G}^a \mathbf{\Gamma}_{R\sigma} \mathbf{G}^r \mathbf{\Gamma}_{L\sigma}\}. \quad (13)$$

In this QD-DTJ system, there exists the tunnel magnetoresistance (TMR) effect, which is caused by the difference between the resistance in parallel and antiparallel configurations of the two FM leads' magnetization. The TMR is given by

$$\text{TMR} = \frac{R^{AP} - R^P}{R^P} = \frac{I^P - I^{AP}}{I^{AP}}, \quad (14)$$

where I^P (I^{AP}) is the tunneling current in parallel (antiparallel) configuration of the two leads' magnetization.

During the course of analyses, we would also consider the state of the QD, which is characterized by its occupancy. The QD's occupancy with electrons of spin- σ can be obtained by considering the lesser Green's function of the QD, i.e.,

$$\langle n_{\sigma} \rangle = \frac{1}{2\pi} \text{Im} \int d\epsilon G_{\sigma,\sigma}^<(\epsilon). \quad (15)$$

2.1.2 Retarded Green's function

To calculate the tunneling current in Eq. (13), one has to obtain the explicit expression for the retarded Green's functions $G_{\sigma,\sigma'}^r(\epsilon)$ of the QD. This can be done by means of the (equation-of-motion) EOM method. By definition, the general form of a retarded Green's function is given by $G_{\sigma,\sigma'}^r(t) = -i\theta(t)\langle\{a_{\sigma}(t), a_{\sigma'}^\dagger\}\rangle$. In the EOM method, the analytical expression for $G_{\sigma,\sigma'}^r(t)$ is obtained by firstly differentiating $G_{\sigma,\sigma'}^r(t)$ with respect to time. This yields

$$\begin{aligned} i\partial_t G_{\sigma,\sigma'}^r(t) &= \delta(t-t')\delta_{\sigma\sigma'} - i\theta(t-t')\langle\{i\partial_t a_{\sigma}(t), a_{\sigma'}^\dagger\}\rangle \\ &= \delta(t-t')\delta_{\sigma\sigma'} - i\theta(t-t')\langle\{-[H, a_{\sigma}], a_{\sigma'}^\dagger\}\rangle. \end{aligned} \quad (16)$$

Based on Eq. (16), for the QD-DTJ system with Hamiltonian in Eq. (1), one may obtain a closed set of equations involving $G_{\sigma,\sigma'}^r(\epsilon)$ after Fourier transform,

$$1 = (\epsilon + i\eta - \epsilon_{\sigma\sigma})G_{\sigma,\sigma}^r - \sum_{v=\{\alpha,k,\sigma'\}} t_{v,\sigma}G_{v,\sigma}^r - \epsilon_{\bar{\sigma}\sigma}G_{\bar{\sigma},\sigma}^r, \quad (17)$$

$$0 = (\epsilon + i\eta - \epsilon_{\bar{\sigma}\bar{\sigma}})G_{\bar{\sigma},\sigma}^r - \sum_{v=\{\alpha,k,\sigma'\}} t_{v,\bar{\sigma}}G_{v,\bar{\sigma}}^r - \epsilon_{\sigma\bar{\sigma}}G_{\sigma,\bar{\sigma}}^r, \quad (18)$$

$$0 = (\epsilon + i\eta - \epsilon_v)G_{v,\sigma}^r - \sum_{\sigma'=\{\sigma,\bar{\sigma}\}} t_{v,\sigma'}^*G_{\sigma',\sigma'}^r, \text{ where } v = \{\alpha,k,\sigma\}, \quad (19)$$

$$0 = (\epsilon + i\eta - \epsilon_v)G_{v,\sigma}^r - \sum_{\sigma'=\{\sigma,\bar{\sigma}\}} t_{v,\sigma'}^*G_{\sigma',\sigma'}^r, \text{ where } v = \{\alpha,k,\bar{\sigma}\}. \quad (20)$$

By solving the equation array of Eqs. (17) to (20), one reaches the explicit expressions for the retarded Green's functions (those in Eq. 12) of the QD:

$$G_{\sigma,\sigma}^r = \frac{1}{\epsilon + i\eta - \epsilon_{\sigma\sigma} - \sum_{\sigma'}^{\sigma} \Sigma_{\sigma\sigma'}^{\sigma}(\epsilon) - \sum_{\bar{\sigma}}^{\bar{\sigma}} \Sigma_{\sigma\bar{\sigma}}^{\bar{\sigma}}(\epsilon) - \frac{\prod_{\sigma'=\{\sigma,\bar{\sigma}\}} \left(\epsilon_{\bar{\sigma}'\sigma'} + \sum_{\sigma''}^{\sigma'} \Sigma_{\sigma'\bar{\sigma}'}^{\sigma'}(\epsilon) + \sum_{\bar{\sigma}''}^{\bar{\sigma}'} \Sigma_{\bar{\sigma}'\sigma''}^{\bar{\sigma}'}(\epsilon) \right)}{\epsilon + i\eta - \epsilon_{\bar{\sigma}\bar{\sigma}} - \sum_{\bar{\sigma}}^{\sigma} \Sigma_{\bar{\sigma}\bar{\sigma}}^{\sigma}(\epsilon) - \sum_{\bar{\sigma}}^{\bar{\sigma}} \Sigma_{\bar{\sigma}\bar{\sigma}}^{\bar{\sigma}}(\epsilon)}}, \quad (21)$$

$$G_{\bar{\sigma},\sigma}^r = \frac{1}{-\epsilon_{\bar{\sigma}\sigma} - \sum_{\bar{\sigma}}^{\sigma} \Sigma_{\bar{\sigma}\bar{\sigma}}^{\sigma}(\epsilon) - \sum_{\bar{\sigma}}^{\bar{\sigma}} \Sigma_{\bar{\sigma}\bar{\sigma}}^{\bar{\sigma}}(\epsilon) + \frac{\prod_{\sigma'=\{\sigma,\bar{\sigma}\}} \left(\epsilon + i\eta - \epsilon_{\bar{\sigma}'\sigma'} - \sum_{\sigma''}^{\sigma'} \Sigma_{\sigma'\bar{\sigma}'}^{\sigma'}(\epsilon) - \sum_{\bar{\sigma}''}^{\bar{\sigma}'} \Sigma_{\bar{\sigma}'\sigma''}^{\bar{\sigma}'}(\epsilon) \right)}{\epsilon_{\sigma\bar{\sigma}} + \sum_{\bar{\sigma}}^{\sigma} \Sigma_{\bar{\sigma}\bar{\sigma}}^{\sigma}(\epsilon) + \sum_{\bar{\sigma}}^{\bar{\sigma}} \Sigma_{\bar{\sigma}\bar{\sigma}}^{\bar{\sigma}}(\omega)}}, \quad (22)$$

where the self energy $\Sigma_{\sigma'\sigma''}^{\sigma}(\epsilon) = \sum_{\{\alpha,k\}} \frac{t_{\alpha k\sigma,\sigma'} t_{\alpha k\sigma,\sigma''}^*}{\epsilon + i\eta - \epsilon_{\alpha k\sigma}}$, $\Sigma_{\sigma'\sigma''}^{\sigma*}(\epsilon) = \sum_{\{\alpha,k\}} \frac{t_{\alpha k\sigma,\sigma'}^* t_{\alpha k\sigma,\sigma''}}{\epsilon + i\eta - \epsilon_{\alpha k\sigma}}$, with $\sigma, \sigma', \sigma'' \in \{\uparrow, \downarrow\}$.

2.2 Results and discussion

Based on the electron transport model developed in Sec. 2.1, one may analyze the SDT properties, such as the spectral functions, the tunneling charge current, spin current, the TMR and the electron occupancies of the QD. The SDT model enables one to investigate the effects of the SF-QD and SF-TJ events and the effect of the coupling asymmetry (CA) on the SDT properties as well.

To focus on the above effects, one may assume that, i) proportional and spin independent lead-QD coupling across the two junctions, i.e., $t_{\alpha k\uparrow,\uparrow} = t_{\alpha k\downarrow,\downarrow} = t_{\alpha k\sigma,\sigma} = t_{\alpha}$, and $t_R = \beta t_L = t$; ii) junction and spin independent strength of SF-TJ, i.e., $t_{\alpha k\uparrow,\downarrow} = t_{\alpha k\downarrow,\uparrow} = t_{\alpha k\sigma,\bar{\sigma}} = v_{\alpha}$, and $v_R = \beta v_L = v$; and iii) spin independence of SF-QD, i.e., $\epsilon_{\uparrow\downarrow} = \epsilon_{\downarrow\uparrow} = \lambda$, iv) the chemical potential of the left and right leads are $\mu_L = 0$, $\mu_R = -eV_b$; and v) spin independence of the energy level of the QD, i.e., $\epsilon_{\sigma\sigma} = \epsilon_{\bar{\sigma}\bar{\sigma}} = \epsilon_d = \epsilon_{d0} - eV_b \frac{\beta^2}{1+\beta^2}$, where ϵ_{d0} is the QD's energy level without bias voltage. Based on the assumptions i)-v) and Eq. (22), one can readily deduce the spin symmetry of the off-diagonal Green's functions, i.e., $G_{\uparrow,\downarrow}^r = G_{\downarrow,\uparrow}^r = G_{\sigma,\bar{\sigma}}^r$. For simplicity, in the following discussion, the form of $G_{\sigma\sigma'}^r$ is used to replace the form of $G_{\sigma,\sigma'}^r$ for retarded Green's function.

2.2.1 Spin-flip effects

Firstly, one may evaluate the four elements of the retarded Green's function (GF) matrix [given in Eq. (12)], $G_{\uparrow\uparrow}^r$, $G_{\uparrow\downarrow}^r$, $G_{\downarrow\uparrow}^r$ and $G_{\downarrow\downarrow}^r$. Based on Eqs. (21) and (22), one may obtain the respective spectral functions, $-2\text{Im}G_{\uparrow\uparrow}^r$, $-2\text{Im}G_{\uparrow\downarrow}^r$, $-2\text{Im}G_{\downarrow\uparrow}^r$, and $-2\text{Im}G_{\downarrow\downarrow}^r$. Spectral functions provide information about the nature of the QD's electronic states which are involved in the tunneling process, regardless whether the states are occupied or not. The spectral functions can be considered as a generalized density of states.

If one neglects the SF-QD or SF-TJ events in the QD-DTJ system, there is no mixing of the spin-up and spin-down electron transport channels. In such QD-DTJ system, the two off-diagonal Green's functions, $G_{\sigma\bar{\sigma}}^r(\sigma = \{\uparrow, \downarrow\})$ become zero [this can be confirmed by considering Eq. (22)], and so are their respective spectral functions. Thus, we focus on the spectral functions corresponding to the diagonal components of the retarded GF matrix. Those spectral functions are analyzed as a function of energy under both parallel and antiparallel configuration of the two FM leads' magnetization, in Figs. 3(a) to (d). A broad peak is observed corresponding to the QD's energy level ($\epsilon = \epsilon_d$). The broad peak can be referred to as "QD resonance". The broadening of the QD resonance is caused by the finite coupling between the QD and the leads, since the QD resonance is a δ function for an isolated QD with no coupling to leads. The width of the QD resonance reflects the strength of coupling between QD and leads; the stronger the coupling is, the broader the energy spread is, hence, a wider peak.

Under zero-bias [shown in Figs. 3 (a) and (b)], one may note three distinct features of the spectral functions:

1. A second resonance peak which corresponds to the leads' potentials, $\mu_L = \mu_R = 0$ eV. The peak can be referred to as the "lead resonance".
2. The lead resonance for the spin-up spectral function ($-2\text{Im}G_{\uparrow\uparrow}^r$) has a broader and lower profile compared to that of the spin-down spectral function, when the QD-DTJ system is in the parallel configuration. This indicates that the excitation at the lead energy has a larger energy spread for spin-up carriers due to the polarization of the lead.
3. The spin-up and spin-down spectral functions are identical in the antiparallel alignment, due to the spin symmetry of the system in antiparallel configuration.

The spectral functions under an finite bias voltage ($V_b = 0.2$ eV) are shown in Figs. 3 (c) and (d). It is observed that,

1. the lead resonance splits into two peaks at the respective left lead and right lead potentials, $\epsilon = \mu_L = 0$ and $\epsilon = \mu_R = -eV_b = -0.2$ eV.
2. In the parallel configuration, the lead resonance of the spin-down electrons is higher (lower) than that of the spin-up electrons at μ_L (μ_R). This is due to the spin-dependence of the electron tunneling between leads and QD.
3. The antiparallel alignment of leads' magnetization gives rise to similar magnitude of the two lead resonances for both spin-up and down spectral functions, due to the spin symmetry of the two spin channels.

Next, one may investigate the SF-TJ effects on the electron transport through the QD-DTJ system, where the SF-TJ strength $v \neq 0$. Figure 4 shows the effect of SF-TJ on the spectral function of diagonal GFs. With the SF-TJ effects, both the QD resonance and the lead

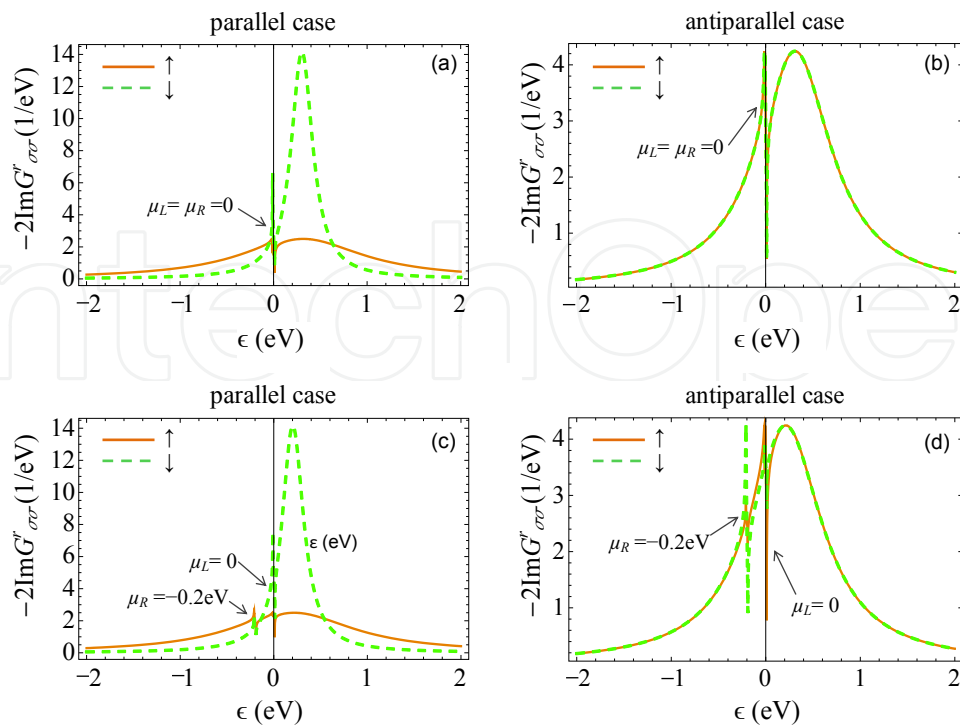


Fig. 3. Spectral functions for spin-up (solid line) and spin-down (dashed line) retarded Green's functions, as a function of electrons' energy, in parallel and antiparallel case. Other parameters are $t=0.5$ eV, $v=0$, $\epsilon_{d0} = 0.3$ eV, $\rho_0 = 0.7(eV)^{-1}$, $p_L = p_R = 0.7$, $\lambda = 0$, $\beta = 1$, $T = 0.3$ K.

resonance at $\epsilon = 0$ are enhanced while the lead resonance at $\epsilon = -eV_b$ is suppressed. This indicates that the increasing SF-TJ helps the tunneling to proceed primarily in the vicinity of the QD's energy level, resulting in an effective decrease in the coupling between the same spin states in leads and QD.

Based on the SDT model, one may analyze the effects of the SF-QD events (denoted by λ) on the spectral functions of the diagonal retarded GFs ($G^r_{\uparrow\uparrow}$ and $G^r_{\downarrow\downarrow}$) of the QD-DTJ system, for both parallel and antiparallel alignments, as shown in Figure 5. At the QD energy level $\epsilon_d = 0.2$ eV, the presence of the SF-QD causes a symmetric split of the QD resonance, resulting in the suppression of tunneling via the lead resonances. The splitting of the QD resonance indicates that the two effective energy levels within the QD are involved in the tunneling process. This split translates to an additional step in the $I - V$ characteristics, which will be discussed later in Fig. 7.

Considering the off-diagonal GF's ($G^r_{\sigma\bar{\sigma}}$), the spectral functions are plotted in Figure 6, for both parallel and antiparallel alignment, under varying SF-TJ strengths (v) and SF-QD strengths (λ). As shown in Figs. 6(a)-(d), without SF-TJ or SF-QD effects, the off-diagonal spectral functions vanish (the solid lines), i.e., the transport proceeds independently in the spin-up and spin-down channels. The presence of either the SF-TJ ($v > 0$) or the SF-QD ($\lambda \neq 0$) enhances the magnitudes of the off-diagonal spectral functions monotonically, indicating stronger mixing of the tunneling transport through the two spin channels.

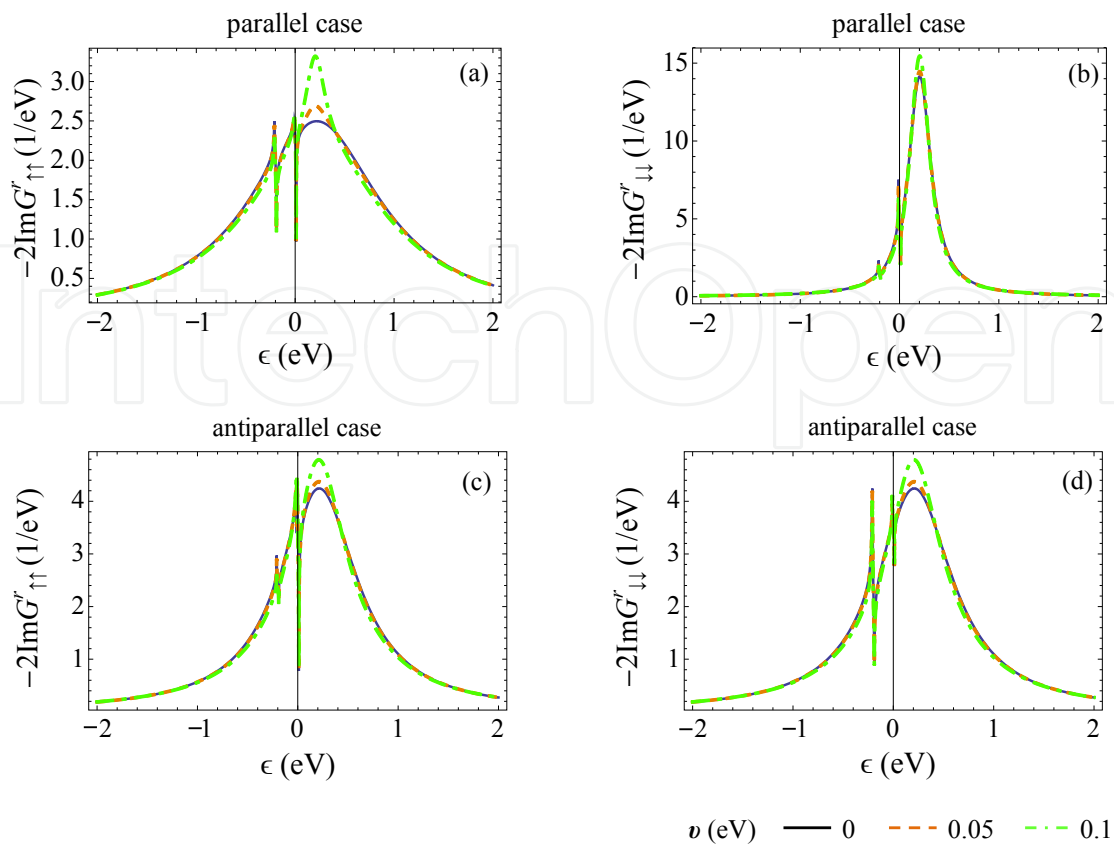


Fig. 4. Spectral functions for the diagonal retarded Green's functions, as a function of electrons' energy, with varied SF-TJ strength (v) between leads and QD, in (a)-(b) parallel and (c)-(d) antiparallel alignment of two leads' magnetization, where $\lambda = 0$ eV, $V_b=0.2$ V. Other parameters are the same with those in Fig. 3.

The individual effects from SF-TJ or SF-QD on the tunneling current and the TMR are then investigated, as shown in Figs. 7.

The $I - V_b$ characteristics in Figs. 7(a)-(b) and Figs. (d)-(e) show a step at the threshold voltage V_{th} , which is required to overcome the Coulomb blockade (CB). The threshold voltage is given by $V_{th} = 2\epsilon_{d0}$. Considering the bias voltage regions, one may find the following features of the $I - V_b$ characteristics,

1. Within the sub-threshold bias range ($V < V_{th}$), the current is still finite due to thermally assisted tunneling at finite temperature.
2. The sub-threshold current is particularly large in the parallel configuration, due to the stronger lead-QD coupling and hence a greater energy broadening of the QD's level.
3. Overall, the parallel current exceeds the antiparallel current for the entire voltage range considered, due to the nonzero spin polarization of the FM lead.
4. Beyond the threshold voltage (i.e. $V_b \gg V_{th}$), the tunneling current saturates since only a single QD level is assumed to participate in the tunneling transport.

In the presence of SF-TJ, the tunneling currents in the parallel and antiparallel configurations are found to be significantly enhanced for bias voltage exceeding the threshold ($V_b > V_{th}$), as shown in Figs. 7(a) and (b). The enhancement in current stems from the overall stronger coupling between the lead and the QD. Additionally, the degree of enhancement of the

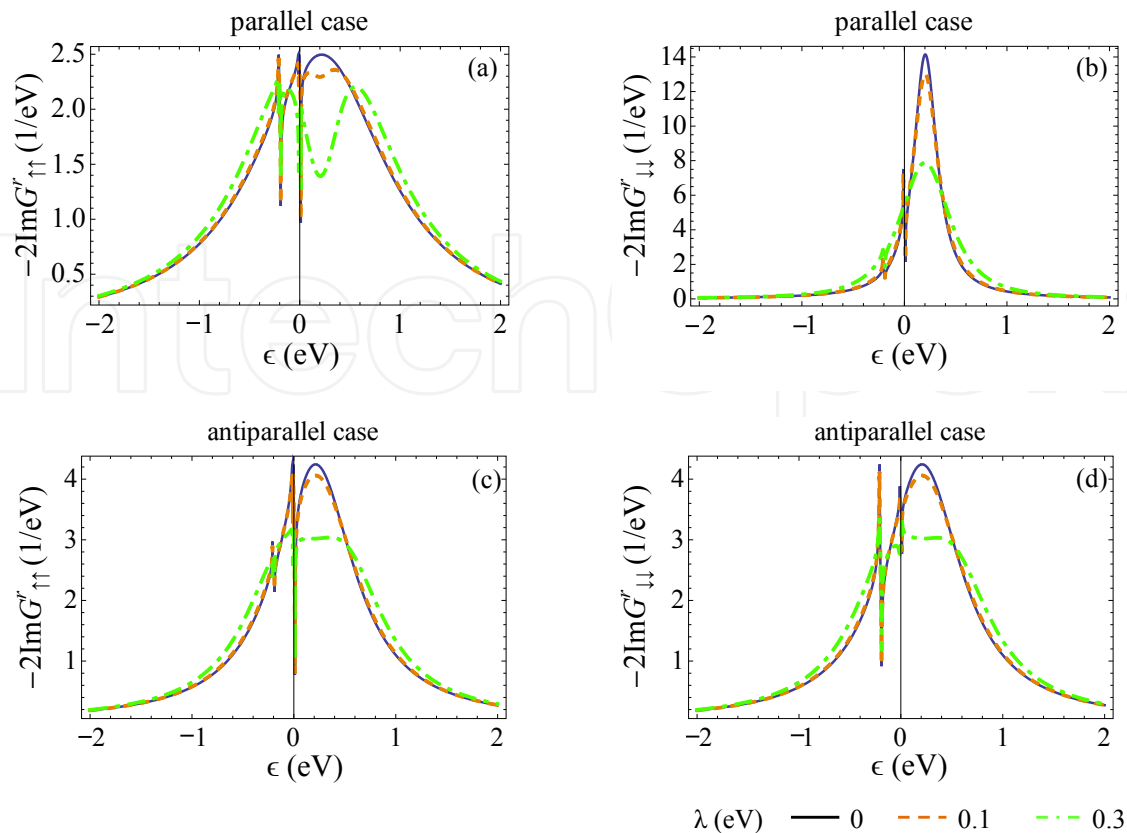


Fig. 5. Spectral function as a function of electrons' energy, with varied SF-QD strength (λ), in (a)-(b) parallel and (c)-(d) antiparallel cases, where $v = 0$ eV. Other parameters are the same with those in Fig. 3.

tunneling current is more pronounced for the parallel alignment of the FM leads. This results in an enhancement of the TMR for the voltage range above the threshold, as shown in Fig. 7(c).

When SF-QD events are present in the system, two new features show up in the $I - V_b$ characteristics, in Figs. 7 (d) and (e). First, the current step at the threshold bias V_{th} splits into two, at $V_b = V_{th} \pm \lambda$, respectively. The presence of the additional step is due to the splitting in the QD resonances observed in the spectral functions of Fig. 5. Secondly, the presence of SF-QD suppresses the current saturation value at large bias voltage (i.e., $V_b \gg V_{th} + \lambda$). The decrease is more pronounced in the antiparallel configuration, resulting in the enhancement of the TMR with the increasing SF-QD probability, as shown in Fig. 7(f).

When both SF processes (Fig. 8) exist in the QD-DTJ system, the two types of SF have competing effects on the tunneling current at large bias voltage exceeding the threshold. The SF-TJ (SF-QD) tends to enhance (suppress) the tunneling current within the bias voltage region exceeding the threshold voltage. This competitive effect is shown for the overall $I - V_b$ characteristics in Figs. 8 (a)-(b). Evidently, the effect caused by one SF mechanism is mitigated by the other for both parallel and antiparallel alignments. However, both SF mechanism contribute to the asymmetry of tunneling current between the parallel and antiparallel cases, leading to an additive effect on the TMR for voltage bias region beyond the threshold voltage, as shown in Fig. 8 (c). The competitive effect on current and collaborative effect on TMR make it possible to attain simultaneously a high TMR and tunneling current density.

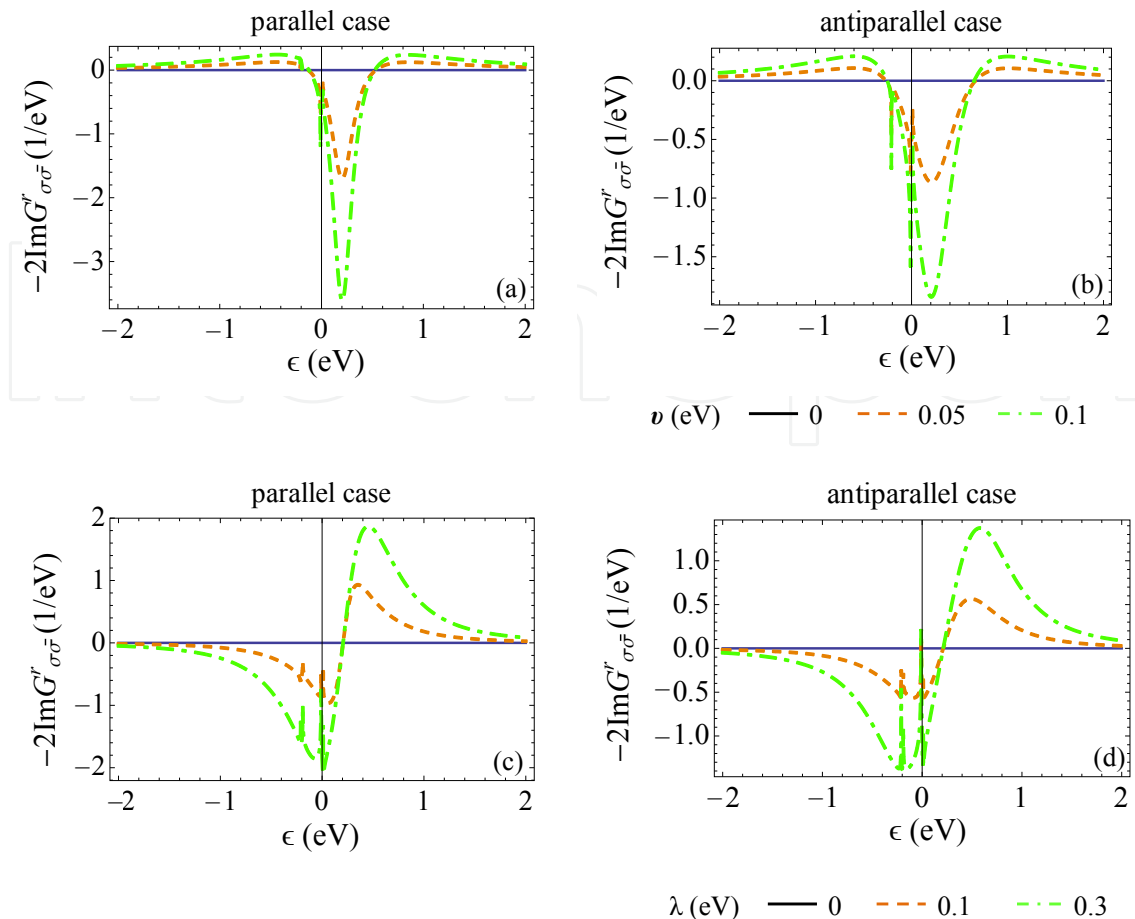


Fig. 6. (a),(b): Off-diagonal spectral functions as a function of energy, for varying SF-TJ strength (ν) between leads and QD, in the absence of SF-QD (i.e., $\lambda = 0$ eV). (c),(d): Off-diagonal Spectral functions as a function of electrons' energy, with varied SF-QD strength (λ), in parallel (left) and antiparallel (right) case, where $\nu=0$ eV. Other parameters are the same with those in Fig. 3.

2.2.2 Coupling asymmetry effects

Recent experimental studies (Hamaya et al. (2009; 2007)) of QD-DTJ structures revealed that the SDT characteristics are strongly dependent on the coupling asymmetry (CA) between the two junctions. Such asymmetry is inherent in the sandwich structure, given the exponential dependence of the coupling strength on the tunnel barrier width.

One may study the effect of the junction CA on the overall spin and charge current characteristics of the QD-DTJ system. The degree of the CA is characterized by the ratio of the right and left junction coupling parameter. The CA is denoted by β and $\beta = t_{Rk\sigma,\sigma}/t_{Lk\sigma,\sigma}$. The spin-up (spin-down) components of the tunneling current can be represented as I_{\uparrow} (I_{\downarrow}), based on which the spin current is defined to be the difference between the two components, $I_s = I_{\uparrow} - I_{\downarrow}$. In the following, one may focus on the parallel alignment of the magnetization of the two leads of the QD-DTJ system, since the magnitude of the spin current is the greatest in this case (see Mu et al. (2006)).

For simplicity but without loss of generality, one may assume β to be spin-independent, i.e., $\beta = t_{Rk\uparrow,\uparrow}/t_{Lk\uparrow,\uparrow} = t_{Rk\downarrow,\downarrow}/t_{Lk\downarrow,\downarrow} = t_{Rk\sigma,\sigma}/t_{Lk\sigma,\sigma}$. In Sec. 2.1, the coupling strength is defined as

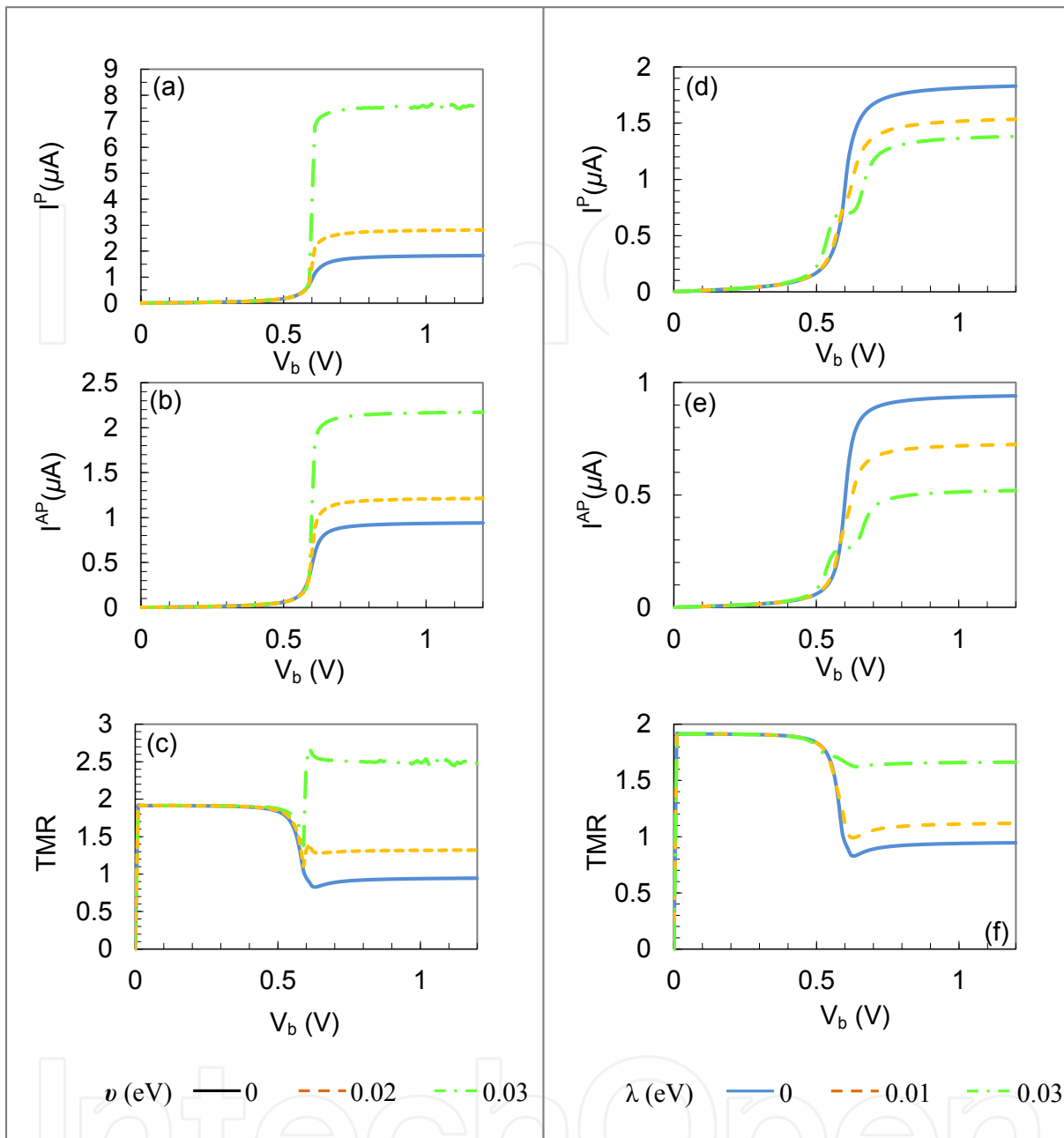


Fig. 7. Current as a function of bias voltage, with varying SF-TJ strength (ν) between the lead and the dot, in (a) parallel and (b) antiparallel cases, or with varying SF-QD strength (λ) in (d) parallel and (e) antiparallel cases. (c)/(f): Tunnel magnetoresistance (TMR) as a function of bias voltage under increasing SF-TJ/SF-QD strength, respectively. In plots (a)-(c), $\lambda=0$ eV, and in plots (d)-(f), $\nu=0$, while other parameters are the same with those in Fig. 3.

$$\Gamma_{\alpha\sigma} = 2\pi\rho_{\alpha\sigma}|t_{\alpha k\sigma,\sigma}^* t_{\alpha k\sigma,\sigma}| = [1 + (-1)^\sigma p_\alpha] 2\pi\rho_{\alpha 0}|t_{\alpha k\sigma,\sigma}^* t_{\alpha k\sigma,\sigma}| = [1 + (-1)^\sigma p_\alpha] \Gamma_{\alpha 0}. \text{ If assuming identical intrinsic electron density of states and identical polarization of the two leads, i.e., } \rho_{\alpha 0} = \rho_0, p_\alpha = p, \text{ one may obtain that } \beta = \sqrt{\Gamma_{R\sigma}/\Gamma_{L\sigma}} = \sqrt{\Gamma_{R0}/\Gamma_{L0}}.$$

We consider the I - V characteristics for the charge current and spin current, shown in Fig. 9 for two different CA values. These two values were chosen so that $\beta_1 = 1/\beta_2$, meaning

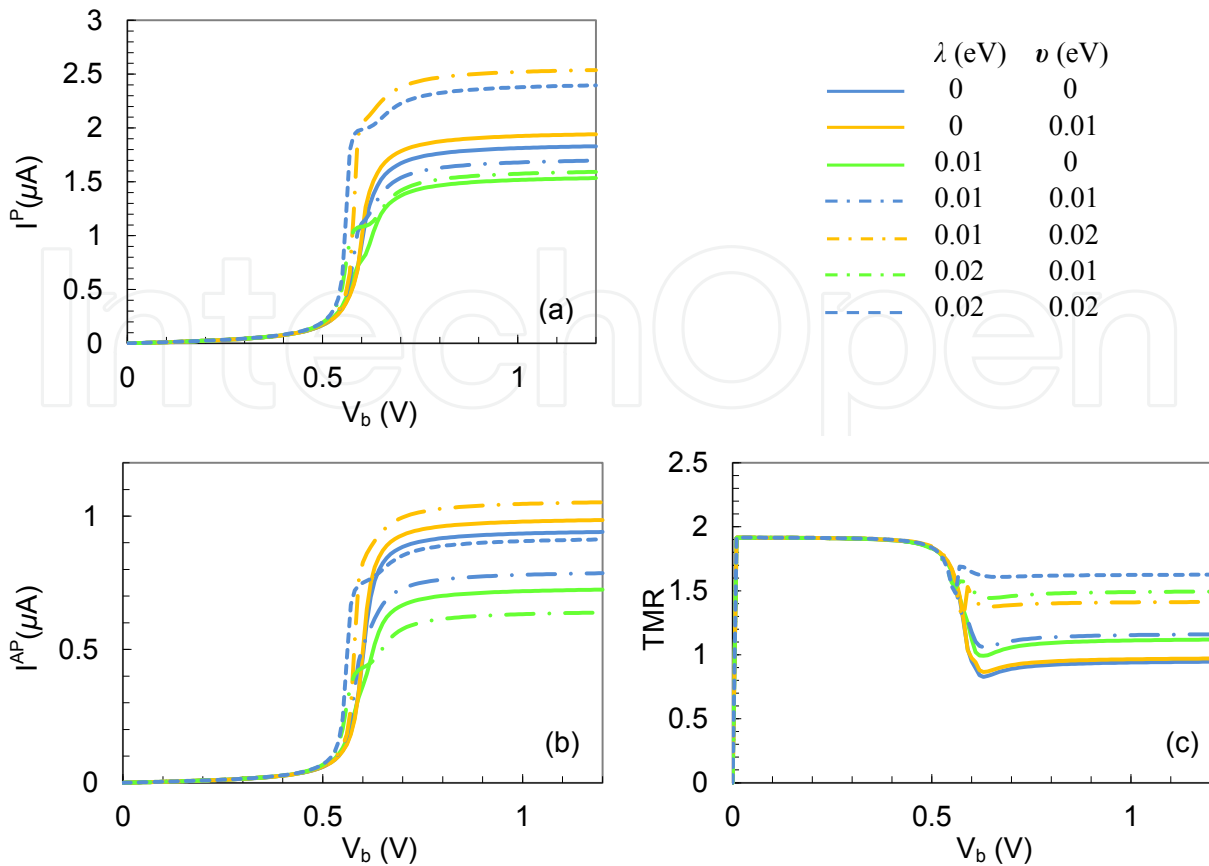


Fig. 8. (a),(b): Current as a function of bias voltage in parallel case and antiparallel case, and (c) TMR as a function of bias voltage, with varying SF-TJ strength (v) and varying SF-QD (λ). Other parameters are the same as those in Fig. 3.

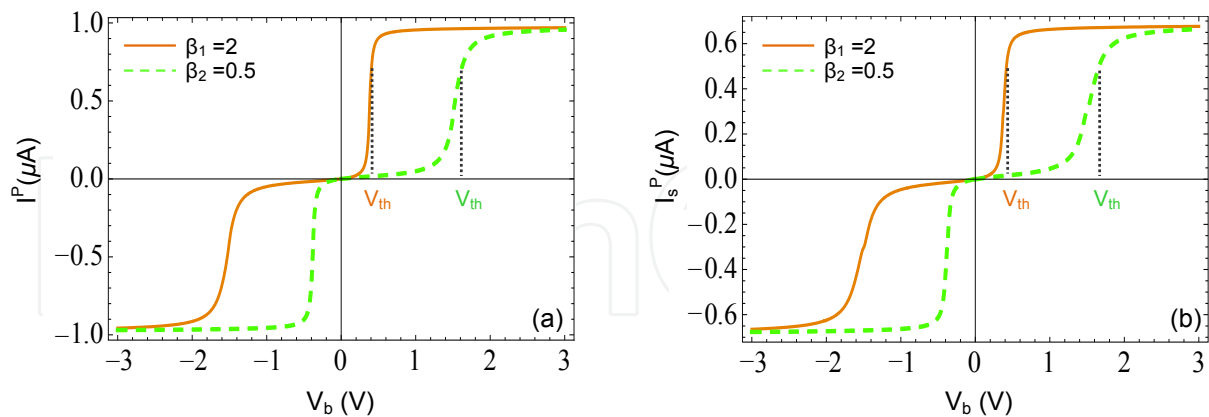


Fig. 9. (a) Charge current I as a function of bias voltage V_b and (b) spin current (I_s) as a function of bias voltage V_b , with two different coupling asymmetry β , in the parallel alignment of the leads' magnetization. The coupling asymmetry is denoted by $\beta = t_{Rk\sigma,\sigma} / t_{Lk\sigma,\sigma} = \sqrt{\Gamma_{R\sigma} / \Gamma_{L\sigma}}$, where $\Gamma_{L\sigma} = (1 \pm p_L)\Gamma_{L0}$ and $\Gamma_{R\sigma} = (1 \pm p_R)\Gamma_{R0}$. Other parameters are $\Gamma_{L0} = 0.012$ eV and $\Gamma_{R0} = \Gamma_{L0} \times \beta_1^2$ for β_1 case, $\Gamma_{L0} = 0.006$ eV and $\Gamma_{R0} = \Gamma_{L0} \times \beta_2^2$ for β_2 case, $\epsilon_{d0} = 0.3$ eV, $p_L = p_R = 0.7$, $T = 100$ K, $v=0$ eV, $\lambda=0$ eV.

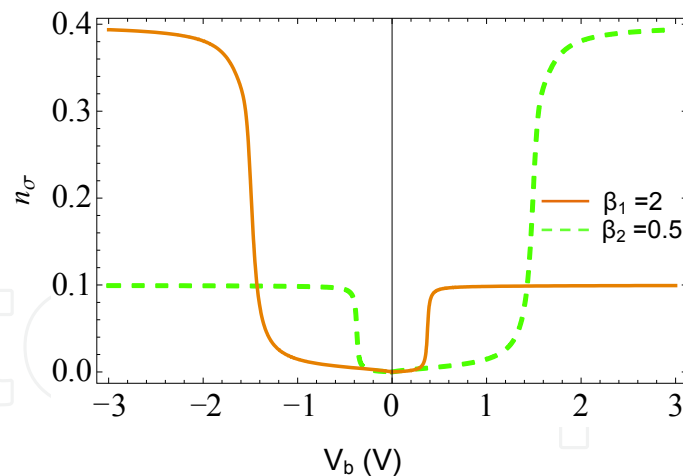


Fig. 10. The occupancy of the quantum dot as a function of bias voltage, with two different coupling asymmetry β , in the parallel alignment of the leads' magnetization. Other parameters are the same with those Fig. 9.

that the left (right) junction in β_1 system is the right (left) junction for β_2 system. It is found that when the coupling strength of the right junction is four times as strong as that of the left junction, i.e., $\beta = 2$, both the magnitude of the charge and spin currents beyond the threshold voltage are the same as those for the reverse case ($\beta = 0.5$). This is due to the fact that the total resistance of the two QD-DTJ system is maintained regardless of the coupling asymmetry reversal. However, the CA affects the threshold voltage V_{th} . This is due to the different shifts of the QD energy level under positive and negative bias voltage, i.e., $V_{th} = 2\epsilon_d$, where $\epsilon_d = \epsilon_{d0} - \frac{\beta^2}{1+\beta^2}eV_b$. The CA effect on the charge current I - V characteristics is consistent with the experimental results observed by K. Hamaya *et al.* for an asymmetric Co/InAs/Co QD-DTJ system (Fig. 2(a) of Ref. Hamaya *et al.* (2007)).

Next, one may investigate the CA effect on the QD occupancies, which are obtained by integrating the spectral function in Eq. (15). The QD occupancies for both spin-up and spin-down electrons are shown in Fig. 10. The occupancies for spin-up and spin-down electrons in the QD actually coincide since the QD-DTJ system is operated in the parallel configuration of the leads' magnetization. Moreover, as β is increased from 0.5 to 2, the QD occupancies of both spin orientations decrease. This decrease is reasonable since as Γ_L is decreased with respect to Γ_R , the coupling which allows the electron to tunnel to the QD from the source (left lead) is reduced, while the coupling which allows the electron to tunnel out of the QD to the drain (right lead) is enhanced. In this circumstance, electrons start to have a higher occupancy in the QD for $\beta < 1$ case, where $\Gamma_L > \Gamma_R$.

2.3 Summary

In summary, the SDT through a QD-DTJ system is theoretically studied. In the SDT model described in Sec.2.1, well-separated QD levels are assumed such that only a single energy level are involved in the SDT process, and the correlation between different energy levels is then neglected. The spectral functions, QD electron occupancies, tunneling charge current, spin current as well as TMR are evaluated based on the Keldysh NEGF formulism and EOM method, with consideration of the effects of the SF-TJ events, SF-QD events, and the CA between the two tunnel junctions on the SDT of the system.

3. QD with Zeeman splitting

In the last section, the SDT is studied for the QD-DTJ system where the spin dependence of the electron transport is caused by the spin polarization in the FM leads. In this section, one may analyze the SDT through the QD-DTJ system where the leads sandwiching the QD are non-magnetic (NM), and a FM gate is applied above the QD. The electron transport through this QD-DTJ system is spin-dependent due to the Zeeman splitting (ZS) generated in the QD. In this QD-DTJ system, one may expect a fully polarized current to tunnel through (Recher et al. (2000)). A fully spin-polarized current is important for detecting or generating single spin states (Prinz (1995; 1998)), and thus is of great importance in the realization of quantum computing (Hanson et al. (2007); Kroutvar et al. (2004); Loss & DiVincenzo (1998); Moodera et al. (2007); Petta et al. (2005); Wabnig & Lovett (2009)).

The QD-DTJ system is schematically shown in Fig. 11. The magnetic field generated by the FM gate is assumed to be spatially localized such that it gives rise to a ZS of the discrete energy levels of the QD, but negligible ZS in the energy levels of the NM electrodes. When the bias voltage V_b between the two NM electrodes, and the size of the ZS in the QD are appropriately tuned, a fully polarized spin current is observed in this QD-DTJ system. The polarization of the current depends on the magnetization direction of the FM gate. Here, the down (up)-spin electrons have spins which are aligned parallel (antiparallel) to the magnetization direction of the FM gate.

3.1 Theory

The Hamiltonian of the QD-DTJ system is in form of

$$H = \sum_{\alpha} H_{\alpha} + H_d + H_t, \quad (23)$$

where

$$H_{\alpha} = \sum_{k\sigma} \epsilon_{\alpha k\sigma} a_{\alpha k\sigma}^{\dagger} a_{\alpha k\sigma}, \quad (24)$$

$$H_d = \sum_{\sigma} \epsilon_{\sigma} a_{\sigma}^{\dagger} a_{\sigma} + U n_{\uparrow} n_{\downarrow}, \quad (25)$$

$$H_t = \sum_{\alpha k\sigma} \left(t_{\alpha k\sigma, \sigma} a_{\sigma}^{\dagger} a_{\alpha k\sigma} + t_{\alpha k\sigma, \sigma}^* a_{\alpha k\sigma}^{\dagger} a_{\sigma} \right), \quad (26)$$

where $\alpha = \{L, R\}$ is the lead index for the left and right leads, k is the momentum, $\sigma = \{\uparrow, \downarrow\}$ is the spin-up and spin-down index, a^{\dagger} and a are the electron creation and annihilation operators, ϵ_{σ} is the energy level in the QD for electrons with spin- σ , U is the Coulomb blockade energy when the QD is doubly occupied by two electrons with opposite spins, and $t_{\alpha k\sigma, \sigma}$ describes the coupling between the electron states with spin- σ in the lead α and the QD.

In our model, we consider only the lowest unoccupied energy level of the QD ϵ_{σ} since most of the overall transport occurs via that level. With the presence of an applied magnetic field B , the lowest unoccupied energy level is given by $\epsilon_{\sigma} = \epsilon_d + \frac{(-1)^{\sigma}}{2} g \mu_B B$, where $\sigma = 0$ ($\sigma = 1$) for up-spin (down-spin) electrons, g is the electron spin g-factor, μ_B is the Bohr magneton, and $g \mu_B B$ is the ZS between the two spin states ϵ_{\downarrow} and ϵ_{\uparrow} . Under an applied bias V_b between the

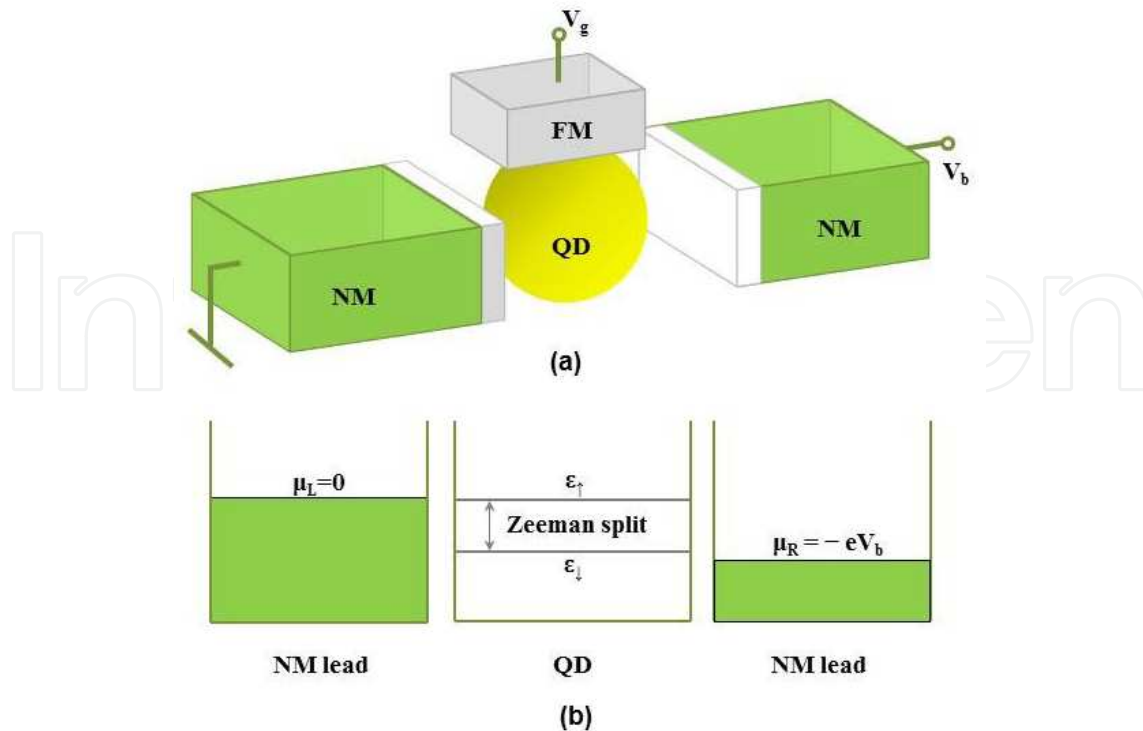


Fig. 11. (a) Schematic diagram of the QD-DTJ set up, which consists of two NM electrodes, one QD and one FM gate. (b) schematic energy diagram of the QD-DTJ system in (a), where V_b is the bias voltage, $\epsilon_\downarrow = \epsilon_d - g\mu_B B/2$ ($\epsilon_\uparrow = \epsilon_d + g\mu_B B/2$) is the energy level for spin-down(up) electrons, respectively, $g\mu_B B$ is the Zeeman splitting between ϵ_\downarrow and ϵ_\uparrow , g is the electron spin g -factor, μ_B is the Bohr magneton, B is the applied magnetic field generated by the FM gate, and $\epsilon_d = \epsilon_{d0} - eV_b\beta^2/(1 + \beta^2)$ is the single energy level of the QD without applied magnetic field, with ϵ_{d0} being the single energy level under zero bias voltage and β being the coupling asymmetry between the two tunnel junctions. We assume a symmetrical QD-DTJ system where $\beta = 1$.

leads and in the absence of B -field, the QD's energy level is modified as $\epsilon_d = \epsilon_{d0} - eV_b\beta^2/(1 + \beta^2)$, where ϵ_{d0} is the energy level at zero bias voltage, and $\beta = t_{Rk\sigma,\sigma}/t_{Lk\sigma,\sigma}$ denotes the asymmetry of the coupling in the left and right tunnel junctions. In the following, a symmetric QD-DTJ system is assumed where $\beta = 1$.

Based on the Hamiltonian, the tunneling current is evaluated via the NEGF formalism introduced in Section. 2.1. The charge and spin current are defined as $I_c = I_\downarrow + I_\uparrow$ and $I_s = I_\downarrow - I_\uparrow$, respectively, where the tunneling current of spin- σ electron tunneling through the QD-DTJ system is given by

$$I_\sigma = \frac{e}{h} \int d\epsilon [f_{L\sigma}(\epsilon) - f_{R\sigma}(\epsilon)] G_{\sigma,\sigma}^a \Gamma_{R\sigma} G_{\sigma,\sigma}^r \Gamma_{L\sigma}. \quad (27)$$

Here, $\Gamma_{\alpha\sigma}(\epsilon) = 2\pi\rho_{\alpha\sigma}(\epsilon)t_{\alpha\sigma,\sigma}(\epsilon)t_{\alpha\sigma,\sigma}^*(\epsilon)$, $G_{\sigma,\sigma}^a(\epsilon) = [G_{\sigma,\sigma}^r(\epsilon)]^*$, $G_{\sigma,\sigma}^r(t) = -i\theta(t)\langle\{a_\sigma(t), a_\sigma^\dagger\}\rangle$.

The explicit form of $G_{\sigma,\sigma}^r(\epsilon)$ is given by

$$G_{\sigma,\sigma}^r(\epsilon) = \frac{1 - n_{\bar{\sigma}}}{\epsilon + i\eta - \epsilon_\sigma - \Sigma(\epsilon)} + \frac{n_{\bar{\sigma}}}{\epsilon + i\eta - \epsilon_{\bar{\sigma}} - \Sigma(\epsilon)}, \quad (28)$$

where the self energy terms are $\Sigma(\epsilon) = \sum_{\{\alpha,k\}} \frac{t_{\alpha k\sigma,\sigma} t_{\alpha k\sigma,\sigma}^*}{\epsilon + i\eta - \epsilon_{\alpha k\sigma}}$. The coupling coefficients $t_{\alpha k\sigma,\sigma}$ and $t_{\alpha k\sigma,\sigma}^*$ are spin-independent since the two leads are NM.

Based on Eqs. (27) and (28), one can then calculate the spin- σ current I_\uparrow and I_\downarrow , and hence the charge and spin current, which are defined as $I_c = I_\downarrow + I_\uparrow$ and $I_s = I_\downarrow - I_\uparrow$, respectively.

In the EOM method, the following Hartree-Fock decoupling approximation of (Lacroix (1981); Sergueev et al. (2002)) is applied,

$$\langle \{ a_{k\alpha\sigma}^\dagger a_\sigma a_{k\alpha\bar{\sigma}}, a_{\bar{\sigma}}^\dagger \} \rangle = \langle a_{k\alpha\sigma}^\dagger a_\sigma \rangle \langle \{ a_{k\alpha\bar{\sigma}} a_{\bar{\sigma}}^\dagger \} \rangle, \quad (29)$$

$$\langle \{ a_\sigma^\dagger a_{k\alpha\sigma} a_{k\alpha\bar{\sigma}}, a_{\bar{\sigma}}^\dagger \} \rangle = \langle a_\sigma^\dagger a_{k\alpha\sigma} \rangle \langle \{ a_{k\alpha\bar{\sigma}} a_{\bar{\sigma}}^\dagger \} \rangle, \quad (30)$$

$$\langle \{ a_\sigma a_{k\alpha\sigma}^\dagger a_{\bar{\sigma}}, a_{\bar{\sigma}}^\dagger \} \rangle \simeq 0, \quad (31)$$

$$\langle \{ a_{k\alpha\sigma} a_\sigma^\dagger a_{\bar{\sigma}}, a_{\bar{\sigma}}^\dagger \} \rangle \simeq 0, \quad (32)$$

$$\langle a_{k\alpha\sigma}^\dagger a_\sigma \rangle = \langle a_\sigma^\dagger a_{k\alpha\sigma} \rangle \simeq 0. \quad (33)$$

3.2 Spin polarized current

Based on the SDT model in Sec. 3.1, one may obtain the $I - V$ characteristics of the system for both spin current I_s and charge current I_c , as shown in Fig. 12.

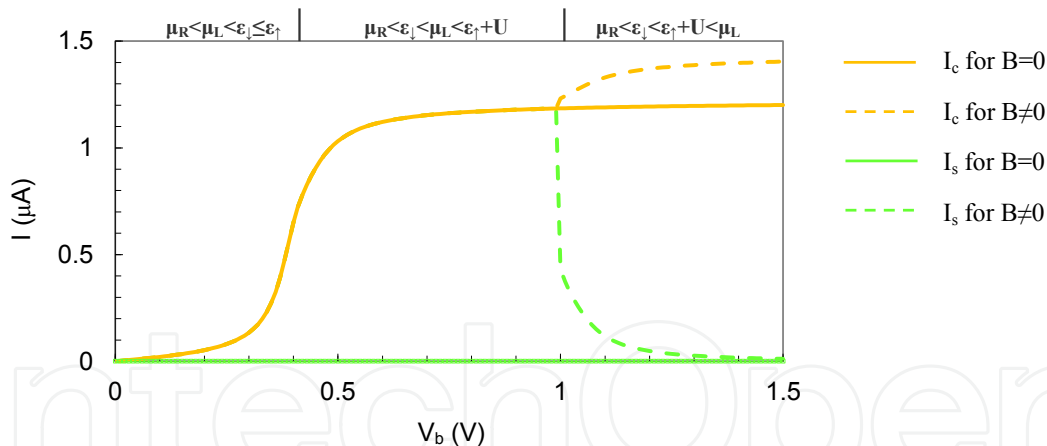


Fig. 12. Charge current (I_c) and spin current (I_s) as a function of the bias voltage, with ($B \neq 0$) or without ($B = 0$) ZS. $V_g = 0$. The following parameters are assumed: lowest unoccupied energy level in the QD under zero bias voltage $\epsilon_{d0} = 0.2 \text{ eV}$, the Coulomb blockade energy $U = 0.26 \text{ eV}$, the Zeeman splitting due to the FM gate is $g\mu_B B = 0(0.36 \text{ meV})$ for $B = 0$ ($B \neq 0$) case, the gate voltage $V_g = 0$, and temperature $T = 3 \text{ K}$.

In the absence of a FM gate, i.e., with zero magnetic field ($B = 0$) applied to the QD, the magnitude of the charge current I_c is the same as that of the system with a FM gate, within the bias region $\mu_R < \epsilon_\downarrow < \mu_L < \epsilon_\uparrow + U$. In this region, the spin current I_s is zero for the system without a FM gate, where the device is spin-symmetric and the transport across it is spin-independent.

For the system with a FM gate, both the charge current I_c and spin current I_s of the system show the three distinct regions with respect to the bias voltage,

1. $\mu_R < \mu_L < \epsilon_{\downarrow} < \epsilon_{\uparrow}$, where both I_c and I_s are negligible due to the suppression of electron tunneling by Coulomb blockade;
2. $\mu_R < \epsilon_{\downarrow} < \mu_L < \epsilon_{\uparrow} + U$, where due to spin blockade, only the spin-down channel contributes to the transport across the system, resulting in a fully spin-down polarized current with $I_s = I_c$;
3. and $\mu_R < \epsilon_{\downarrow} < \epsilon_{\uparrow} + U < \mu_L$, where it is energetically favorable for both types of spins to tunnel across the device, leading to zero spin current.

The sign of the spin polarization of the tunneling current can be *electrically* modulated, i.e., by means of a gate voltage V_g . The gate voltage modulation of the QD energy level ϵ_d can result in the switching of the spin polarization of current, without requiring any corresponding change to the magnetization of the FM gate. If the energy diagram of the system satisfies $\epsilon_{\downarrow} - eV_g < \mu_R < \epsilon_{\uparrow} - eV_g < \mu_L$, a fully spin-up polarized current will thus flow continuously through the system.

3.3 Summary

In summary, the SDT through a QD-DTJ system is analyzed with NM leads and FM gate. Under the applied magnetic field from the FM gate, the energy level in the QD splits to two due to ZS effect. The two energy levels can be modulated by the gate voltage applied to the FM gate. Based on the SDT model developed by NEGF formalism and EOM method, the $I - V_b$ characteristics is analyzed, and a fully spin-down polarized current is obtained when the system is operated under a proper bias voltage between the two leads. Additionally, by utilizing the gate voltage modulation instead of switching the magnetization of the FM gate, the polarization of the current can be reversed from spin-down to spin-up by electrical means.

4. Conclusion

In conclusion, the SDT is theoretically studied for the QD-DTJ systems where a QD is sandwiched by two adjacent leads. The tunneling current through the systems is shown to be rigorously derived via the Keldysh NEGF approach and EOM method. The SF events, CA, ZS and FM gating are systematically incorporated in the SDT models. Considering these effects, one may analyze the SDT properties of QD-DTJ systems, including the tunneling current (charge current and spin current), the TMR, the spectral functions and the occupancies of the QD. The SF-TJ and the SF-QD events are found to have competitive effects on the tunneling current. The presence of CA effectively modifies the threshold voltage, and gives rise to additional bias voltage dependence of the QD's electron occupancy and the charge and spin currents. The FM gate attached to the QD can be utilized to generate a bipolar spin polarization of the current through QD-DTJ systems. The above investigations done have yielded a better understanding of the SDT in QD-DTJ systems.

5. Acknowledgement

We gratefully acknowledge the SERC Grant No. 092 101 0060 (R-398-000-061-305) for financially supporting this work.

6. List of Abbreviations

CA	coupling asymmetry
CB	Coulomb blockade
DOS	density of states
DTJ	double tunnel junction
EOM	equation of motion
FM	ferromagnetic
GF	Green's function
ME	master equation
NEGF	nonequilibrium Green's function
NM	non-magnetic
QD	quantum dot
SDT	spin dependent transport
SF	spin-flip
TMR	tunnel magnetoresistance
ZS	Zeeman splitting

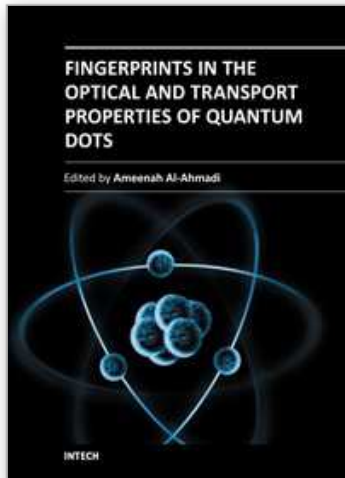
7. References

- Bao, Y. J., Tong, N. H., Sun, Q. F. & Shen, S. Q. (2008). Conductance plateau in quantum spin transport through an interacting quantum dot, *Europhys. Lett.* 83: 37007:1–5.
- Braig, S. & Brouwer, P. W. (2005). Rate equations for coulomb blockade with ferromagnetic leads, *Phys. Rev. B* 71: 195324:1–9.
- Bruus, H. & Flensberg, K. (2004). *Many-body Quantum Theory in Condensed Matter Physics*, Oxford University Press, New York.
- Caroli, C., Combescot, R., Nozieres, P. & Saint-James, D. (1971). Direct calculation of the tunneling current, *J. Phys. C* 4: 916.
- Deshmukh, M. M. & Ralph, D. C. (2002). Using single quantum states as spin filters to study spin polarization in ferromagnets, *Phys. Rev. Lett.* 89: 266803:1–4.
- Fransson, J. & Zhu, J.-X. (2008). Spin dynamics in a tunnel junction between ferromagnet, *New J. Phys.* 10: 013017:1–9.
- Hamaya, K., Kitabatake, M., Shibata, K., Jung, M., Ishida, S., Taniyama, T., Hirakawa, K., Arakawa, Y. & Machida, T. (2009). Spin-related current suppression in a semiconductor quantum dot spin-diode structure, *Phys. Rev. Lett.* 102: 236806:1–4.
- Hamaya, K., Masubuchi, S., Kawamura, M., Machida, T., Jung, M., Shibata, K., Hirakawa, K., Taniyama, T., Ishida, S. & Arakawa, Y. (2007). Spin transport through a single self-assembled inas quantum dot with ferromagnetic leads, *Appl. Phys. Lett.* 90: 053108.
- Hanson, R., Kouwenhoven, L. P., Petta, J. R., Tarucha, S. & Vandersypen, L. M. K. (2007). *Rev. Mod. Phys.* 79: 1217.

- Jauho, A. P., Wingreen, N. S. & Meir, Y. (1994). Time-dependent transport in interacting and noninteracting resonant-tunneling systems, *Phys. Rev. B* 50: 5528–5544.
- Katsura, H. (2007). Nonequilibrium kondo problem with spin-dependent chemical potentials: Exact results, *J. Phys. Soc. Jpn* 76: 054710.
- Kroutvar, M., Ducommun, Y., Heiss, D., Bichler, M., Schuh, D., Abstreiter, G. & Finley, J. J. (2004). Optically programmable electron spin memory using semiconductor quantum dots, *Nature* 432: 81–84.
- Kuo, D. M. T. & Chang, Y. (2007). Tunneling current spectroscopy of a nanostructure junction involving multiple energy levels, *Phys. Rev. Lett.* 99: 086803:1–4.
- Lacroix, C. (1981). Density of states for the anderson model, *J. Phys. F: Met. Phys.* 11: 2389.
- Lin, K.-C. & D.-S.Chuu (2005). Anderson model with spin-flip-associated tunneling, *Phys. Rev. B* 72: 125314:1–11.
- Lobo, T., Figueira, M. S. & Foglio, M. E. (2006). Kondo effect in a quantum dot-the atomic approach, *Nanotechnology* 17: 6016.
- Loss, D. & DiVincenzo, D. P. (1998). Quantum computation with quantum dots, *Phys. Rev. A* 57: 120–126.
- Ma, M. J., Jalil, M. B. A. & Tan, S. G. (2008). Sequential tunneling through a two-level semiconductor quantum dot system coupled to magnetic leads, *J. Appl. Phys.* 104: 053902:1–6.
- Ma, M. J., Jalil, M. B. A. & Tan, S. G. (2010). Coupling asymmetry effect on the coherent spin current through a ferromagnetic lead/quantum dot/ferromagnetic lead system, *IEEE Trans. Magnetics* 46: 1495.
- Mahan, G. D. (1990). *Many-Particle Physics*, 2nd edn, Plenum, New York.
- Manassen, Y., Mukhopadhyay, I. & Rao, N. R. (2001). Electron-spin-resonance stm on iron atoms in silicon, *Phys. Rev. B* 61: 16223–16228.
- Meir, Y. & Wingreen, N. S. (1992). Landauer formula for the current through an interacting electron region, *Phys. Rev. Lett.* 68: 2512–2515.
- Meir, Y., Wingreen, N. S. & Lee, P. A. (1991). Transport through a strongly interacting electron system: Theory of periodic conductance oscillations, *Phys. Rev. Lett.* 66: 3048–3051.
- Meir, Y., Wingreen, N. S. & Lee, P. A. (1993). Low-temperature transport through a quantum dot: The anderson model out of equilibrium, *Phys. Rev. Lett.* 70: 2601–2604.
- Moodera, J. S., Santos, T. S. & Nagahama, T. (2007). The phenomena of spin-filter tunnelling, *J. Phys.: Condens. Matter* 19: 165202.
- Mu, H. F., Su, G. & Zheng, Q. R. (2006). Spin current and current-induced spin transfer torque in ferromagnet-quantum dot-ferromagnet coupled systems, *Phys. Rev. B* 73: 054414:1–9.
- Pasupathy, A., Bialczak, R., Martinek, J., Grose, J., Donev, L., McEuen, P. & Ralph, D. C. (2004). The kondo effect in the presence of ferromagnetism, *Science* 306: 86–89.
- Petta, J. R., Johnson, A. C., Taylor, J. M., Laird, E. A., Yacoby, A., Lukin, M. D., Marcus, C. M., Hanson, M. P. & Gossard, A. C. (2005). Coherent manipulation of coupled electron spins in semiconductor quantum dots, *Science* 309: 2180–2184.
- Potok, R. M., Rau, I. G., Shtrikman, H., Oreg, Y. & Goldhaber-Gordon, D. (2007). Observation of the two-channel kondo effect, *Nature* 446: 167–171.
- Prinz, G. (1995). Spin-polarized transport, *Phys. Today* 48: 58.
- Prinz, G. (1998). Magnetoelectronics, *Science* 282: 1660–1663.

- Qi, Y., Zhu, J.-X., Zhang, S. & S.Ting, C. (2008). Kondo resonance in the presence of spin-polarized currents, *Phys. Rev. B* 78: 045305:1–5.
- Qu, F. & Vasilopoulos, P. (2006). Spin transport across a quantum dot doped with a magnetic ion, *Appl. Phys. Lett.* 89: 122512:1–3.
- Recher, P., Sukhorukov, E. V. & Loss, D. (2000). Quantum dot as spin filter and spin memory, *Phys. Rev. Lett.* 85: 1962–1965.
- Rudziński, W. & Barnaś, J. (2001). Tunnel magnetoresistance in ferromagnetic junctions: Tunneling through a single discrete level, *Phys. Rev. B* 64: 085318:1–10.
- Sergueev, N., Sun, Q. F., Guo, H., Wang, B. G. & Wang, J. (2002). Spin-polarized transport through a quantum dot: Anderson model with on-site coulomb repulsion, *Phys. Rev. B* 65: 165303.
- Shaji, N., Simmons, C. B., Thalakulam, M., Klein, L. J., Qin, H., Luo, H., Savage, D. E., Lagally, M. G., Rimberg, A. J., Joynt, R., Friesen, M., Blick, R. H., Coppersmith, S. N. & Eriksson, M. A. (2008). Spin blockade and lifetime-enhanced transport in a few-electron si/sige double quantum dot, *Nature Physics* 4: 540–544.
- Souza, F. M., Egues, J. C. & Jauho, A. P. (2004). Tmr effect in a fm-qd-fm system, *Brazilian Journal of Physics* 34: 565–567.
- Wabnig, J. & Lovett, B. W. (2009). A quantum dot single spin meter, *New J. Phys.* 11: 043031.
- Weymann, I. & Barnaś, J. (2007). Cotunneling through quantum dots coupled to magnetic leads: Zero-bias anomaly for noncollinear magnetic configurations, *Phys. Rev. B* 75: 155308:1–12.
- Zhang, P., Xue, Q. K., Wang, Y. P. & Xie, X. C. (2002). Spin-dependent transport through an interacting quantum dot, *Phys. Rev. Lett.* 89: 286803:1–4.
- Zhu, J.-X. & Balatsky, A. V. (2002). Quantum electronic transport through a precessing spin, *Phys. Rev. Lett.* 89: 286802:1–4.

IntechOpen



Fingerprints in the Optical and Transport Properties of Quantum Dots

Edited by Dr. Ameenah Al-Ahmadi

ISBN 978-953-51-0648-7

Hard cover, 468 pages

Publisher InTech

Published online 13, June, 2012

Published in print edition June, 2012

The book "Fingerprints in the optical and transport properties of quantum dots" provides novel and efficient methods for the calculation and investigating of the optical and transport properties of quantum dot systems. This book is divided into two sections. In section 1 includes ten chapters where novel optical properties are discussed. In section 2 involve eight chapters that investigate and model the most important effects of transport and electronics properties of quantum dot systems This is a collaborative book sharing and providing fundamental research such as the one conducted in Physics, Chemistry, Material Science, with a base text that could serve as a reference in research by presenting up-to-date research work on the field of quantum dot systems.

How to reference

In order to correctly reference this scholarly work, feel free to copy and paste the following:

Minjie Ma, Mansoor Bin Abdul Jalil and Seng Ghee Tan (2012). Coherent Spin Dependent Transport in QD-DTJ Systems, Fingerprints in the Optical and Transport Properties of Quantum Dots, Dr. Ameenah Al-Ahmadi (Ed.), ISBN: 978-953-51-0648-7, InTech, Available from: <http://www.intechopen.com/books/fingerprints-in-the-optical-and-transport-properties-of-quantum-dots/coherent-spin-dependent-transport-in-quantum-dot-systems>

INTECH
open science | open minds

InTech Europe

University Campus STeP Ri
Slavka Krautzeka 83/A
51000 Rijeka, Croatia
Phone: +385 (51) 770 447
Fax: +385 (51) 686 166
www.intechopen.com

InTech China

Unit 405, Office Block, Hotel Equatorial Shanghai
No.65, Yan An Road (West), Shanghai, 200040, China
中国上海市延安西路65号上海国际贵都大饭店办公楼405单元
Phone: +86-21-62489820
Fax: +86-21-62489821

© 2012 The Author(s). Licensee IntechOpen. This is an open access article distributed under the terms of the [Creative Commons Attribution 3.0 License](#), which permits unrestricted use, distribution, and reproduction in any medium, provided the original work is properly cited.

IntechOpen

IntechOpen